

**AD-A268 975**



2

**PL-TR-92-2168**

**Instrumentation Papers, No. 344**

**EFFECTS OF MAGNUS MOMENTS ON  
MISSILE AERODYNAMIC PERFORMANCE**

**George Y. Jumper, Jr  
C. J. Frushon, Capt, USAF  
R. K. Longstreth, Capt, USAF  
J. Smith, Capt, USAF  
J. Willett  
D. Curtis**

**DTIC  
ELECTE  
AUG 24 1993**

**10 December 1991**

**APPROVED FOR PUBLIC RELEASE; DISTRIBUTION UNLIMITED**



**PHILLIPS LABORATORY  
Directorate of Geophysics  
AIR FORCE SYSTEMS COMMAND  
HANSCOM AIR FORCE BASE, MA 01731-5000**

98 8 23 024

**93-19531**



"This technical report has been reviewed and is approved for publication"



---

EDWARD F. MCKENNA, Chief  
System Integration Branch  
Aerospace Engineering Division



---

C. NEALON STARK, Director  
Aerospace Engineering Division

This report has been reviewed by the ESD Public Affairs Office (PA) and is releasable to the National Technical Information Service (NTIS).

Qualified requestors may obtain additional copies from the Defense Technical Information Center. All others should apply to the National Technical Information Service.

If your address has changed, or if you wish to be removed from the mailing list, or if the addressee is no longer employed by your organization, please notify PL/IMA, Hanscom AFB, MA 01731. This will assist us in maintaining a current mailing list.

# REPORT DOCUMENTATION PAGE

Form Approved  
OMB No. 0704-0188

Public reporting burden for this collection of information is estimated to average 1 hour per response, including the time for reviewing instructions, searching existing data sources, gathering and maintaining the data needed, and completing and reviewing the collection of information. Send comments regarding this burden estimate or any other aspect of this collection of information, including suggestions for reducing this burden, to Washington Headquarters Services, Directorate for Information Operations and Reports, 1215 Jefferson Davis Highway, Suite 1204, Arlington, VA 22202-4302, and to the Office of Management and Budget, Paperwork Reduction Project (0704-0188), Washington, DC 20503.

<b>1. AGENCY USE ONLY (Leave blank)</b>	<b>2. REPORT DATE</b> 10 December 1991	<b>3. REPORT TYPE AND DATES COVERED</b> Scientific, Final	
<b>4. TITLE AND SUBTITLE</b> Effects of Magnus Moments on Missile Aerodynamic Performance		<b>5. FUNDING NUMBERS</b> PE 62101F PR 6670. TA 12 WU 12	
<b>6. AUTHOR(S)</b> George Y. Jumper, Jr*; Cl J. Frushon, Capt, USAF; R. K. Longstreth, Capt, USAF; J. Smith, Capt, USAF; J. Willett; D. Curtis			
<b>7. PERFORMING ORGANIZATION NAME(S) AND ADDRESS(ES)</b> Phillips Laboratory (SXAI) Hansccm AFB, MA 01731-5000		<b>8. PERFORMING ORGANIZATION REPORT NUMBER</b> PL-TR-92-2168 IP, No. 344	
<b>9. SPONSORING/MONITORING AGENCY NAME(S) AND ADDRESS(ES)</b> Air Force Office of Scientific Research Air Force Systems Command, USAF (and) Phillips Laboratory Hanscom AFB, MA 01731-5000		<b>10. SPONSORING/MONITORING AGENCY REPORT NUMBER</b>	
<b>11. SUPPLEMENTARY NOTES</b>  *AFOSR Summer Research Fellow, 1990			
<b>12a. DISTRIBUTION/AVAILABILITY STATEMENT</b>  APPROVED FOR PUBLIC RELEASE; DISTRIBUTION IS UNLIMITED		<b>12b. DISTRIBUTION CODE</b>	
<b>13. ABSTRACT (Maximum 200 words)</b>  A 3 degree of freedom computer simulation was used to study a new configuration of the 2.75" Folding Fin Aircraft Rocket (FFAR) designed to carry the payload for the REFS (Rocket Electric Field Sounding) program. Since the shell of the payload section of the new configuration spins at a different rate than the motor casing, relatively large moments from the Magnus forces have some effect on the aerodynamic characteristics of the missile. Aerodynamic coefficients were based on existing flight data of the FFAR and predictions of the USAF Missile DATCOM program.			
<b>14. SUBJECT TERMS</b> Magnus effect, Sounding rocket, 3 degree of freedom, Euler angles		<b>15. NUMBER OF PAGES</b> 36	
		<b>16. PRICE CODE</b>	
<b>17. SECURITY CLASSIFICATION OF REPORT</b> UNCLASSIFIED	<b>18. SECURITY CLASSIFICATION OF THIS PAGE</b> UNCLASSIFIED	<b>19. SECURITY CLASSIFICATION OF ABSTRACT</b> UNCLASSIFIED	<b>20. LIMITATION OF ABSTRACT</b> SAR

# Contents

1	INTRODUCTION	1
2	THEORY	2
2.1	Rotational Motion: . . . . .	2
2.2	The Moments . . . . .	9
2.2.1	Roll Moments: . . . . .	9
2.2.2	Pitch and Yaw Moments: . . . . .	9
2.2.3	Magnus Moments . . . . .	12
2.3	Solution of Equations of Rotation . . . . .	17
3	RESULTS	18
4	CONCLUSIONS	28
	References	29

DTIC QUALITY INSPECTED 3

<b>Accession For</b>	
NTIS GRA&I	<input checked="" type="checkbox"/>
DTIC TAB	<input type="checkbox"/>
Unannounced	<input type="checkbox"/>
Justification	
By _____	
Distribution/	
Availability Codes	
Dist	Avail and/or Special
A-1	

## List of Figures

1	The REFS Missile . . . . .	3
2	The Yaw-Pitch Euler Angle Coordinate System . . . . .	5
3	The Angular Velocities in the Yaw-Pitch Euler Angle Coordinate System . . . . .	6
4	Predicted Roll Output Compared to the Data of Winn . . . . .	10
5	Magnus Lift and Drag Figure from Reference 9, Originally From Reference 10, With the Curve Fits Through the Experimental Data Used for This Study . . . . .	13
6	Elevation View of the Pitch Plane and Normal View in the Pitch Plane of the REFS Missile Showing Magnus Lift and Drag Forces . . . . .	16
7	Pitch Plane Moments on the REFS Missile With Positive Forward Section Rotation as a Function of Time . . . . .	19
8	Pitch Plane Moments on the REFS Missile With Negative Forward Section Rotation as a Function of Time . . . . .	20
9	Total Angle of Attack Versus Time With Positive and Negative Forward Section Rotation . . . . .	21
10	Total Angle of Attack for Two Values of Static Margin for Both Positive and Negative Angle Forward Section Rotation . . . . .	23
11	Euler Angle $\theta$ vs Euler Angle $\psi$ for Positive and Negative Forward Section Rotation . . . . .	24
12	The Bank-Pitch Euler Angle Coordinate System . . . . .	25

## List of Tables

1	Parameters for REFS System Analysis . . . . .	18
---	---	----

## Acknowledgements

Research sponsored by the Air Force Office of Scientific Research, Air Force Systems Command, United States Air Force, under contract F49620-88-C-0053 to UES, Inc., Dayton, Ohio. The United States Government is authorized to reproduce and distribute reprints for governmental purposes notwithstanding any copyright notation hereon. The authors want acknowledge the support of G. Kirpa, R. Steves and C. N. Stark. Also, we are indebted to Prof. Raymond Hagglund for insight into the world of Euler angles, and M.J. McCrossan for the art work.

# Effects of Magnus Moments on Missile Aerodynamic Performance

## 1 INTRODUCTION

The goal of the atmospheric research program, Rocket Electric Field Sounding (REFS), is to determine the minimum electrical field strength that would pose a lightning strike hazard to ascending rockets such as the Space Shuttle. The 2.75-in. Folding Fin Aircraft Rocket (FFAR) was selected to carry the scientific payload. The FFAR missile is aerodynamically unstable at launch, until the fins spring out. To minimize the effects of the instability, several versions of the missile have nozzle designs that provide a roll moment during thrust. When a spinning cylindrical body experiences any pitch or yaw to the local windstream, a side force is produced which is proportional to both the angle of yaw and the angular velocity of the spin. This is the well known Magnus effect. If the center of pressure for this force is too far from the center of mass, the resulting moments can cause the projectile to be dynamically unstable.<sup>1</sup>

The FFAR configuration, which will be used for the REFS experiment, has the potential for higher than normal moments from the Magnus forces due to the fact that the outer shell of the payload section of the missile is designed to spin at a rate that is different from the rate of the rearward portion of the missile, as shown in Figure 1. The net effect is that any pitch or yaw of the missile produces magnus forces of different magnitudes for each portion of the body, resulting in a moment on the missile.

The purpose of this study is to perform an approximate analysis of the rotational motion of the REFS missile to determine the potential for instability

---

Received for publication 1 July 1992

due to the Magnus moments.

## 2 THEORY

The motion of a vehicle in flight is governed by Newton's Laws of motion, which strictly apply to each point mass that makes up the object. When these laws are properly applied to each infinitesimal portion of the body, the total effect on a rigid body can be represented by three scalar equations of linear motion of the center of mass of the vehicle and three scalar equations of rotational motion of the body about the center of mass. An analysis that considers both linear and rotational motion is known as a six degree of freedom analysis (6DOF). There are several computer models that perform this complete analysis (for example, MASS);<sup>2</sup> however, these complete simulations are often complex and difficult to use to isolate specific cause and effect relationships.

For this work, only the rotational motion will be analyzed. The magnitude of the velocity of the missile is considered an independent variable which is specified to vary with time in a way similar to that observed in test flights. The velocity vector is assumed to always point in the same direction and missile rotations are analyzed relative to this fixed direction. This simplification differs from reality in two important ways. First, the change in velocity direction as a vehicle moves along the trajectory provides a continual forcing function to change the angular position of the vehicle. In this regard, the analysis can be considered incomplete and possibly non-conservative since a perturbation is usually only introduced at the start of the analysis and, if it damps out, the vehicle is assumed stable. Second, this analysis ignores the effect that angular position relative to the velocity vector has on the velocity itself. For a reasonable missile vehicle which does not experience very large divergence angles from the velocity vector, this is not a problem except for the thrusting phase of flight. While thrusting, the vehicle, in effect, reduces angular divergences by causing changes to velocity to be in the direction of the flight vehicle if the rocket nozzles are aligned with the missile. Consequently, the angular motions predicted during thrusting are larger than those that would be actually experienced in flight.

### 2.1 Rotational Motion:

The equations governing the rotational motion about the center of mass of an object are known as Euler's Equations.<sup>3</sup> The three scalar components are represented by the single vector equation:

$$\mathbf{M}_{cm} = \dot{\mathbf{H}}_{cm} \quad (1)$$

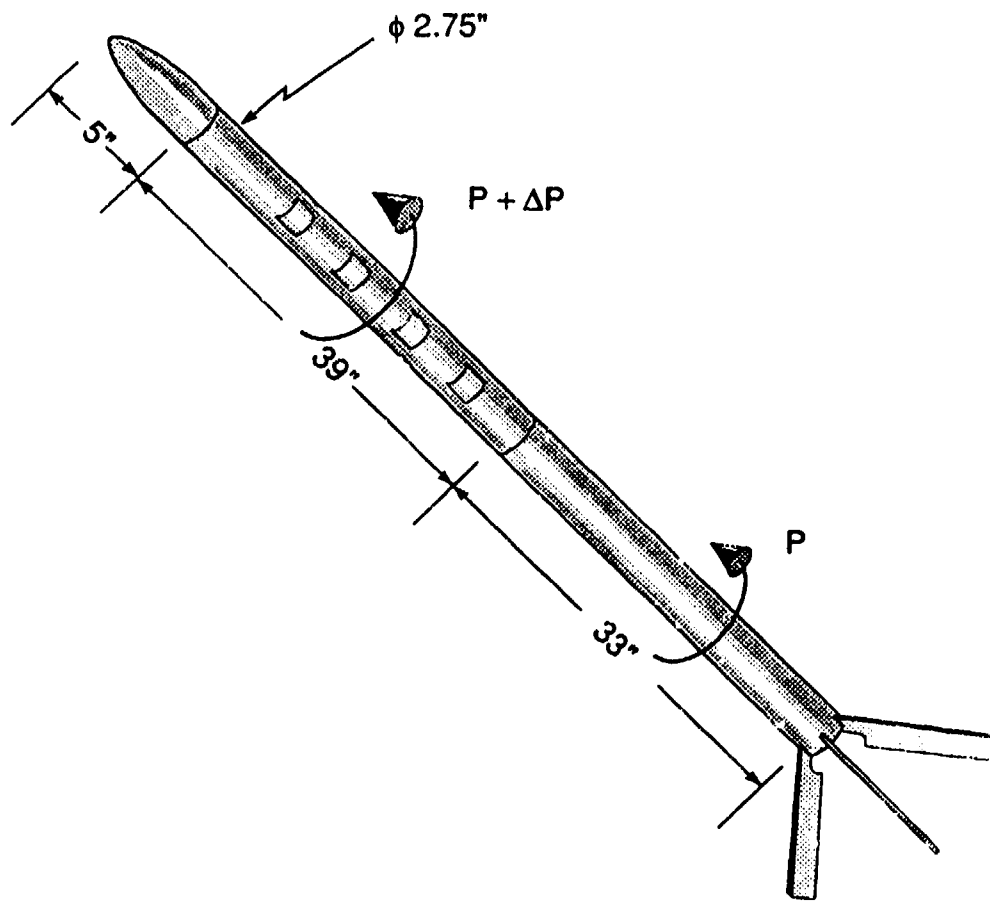


Figure 1: The REFS Missile

where

$M_{cm}$  is the moment about the center of mass,

and

$\dot{H}_{cm}$  is the time derivative of the angular momentum vector about the center of mass.

The change in the  $H$  vector must be with respect to either an inertial coordinate system or a non-rotating coordinate system through the center of mass of the body. The latter is most often used for analysis of flight systems. The forces and moments experienced by a flight vehicle are usually expressed in terms of a coordinate system that is fixed to and rotating with the vehicle. Consequently, it is not convenient to express these forces and moments in terms of a non-rotating system. The equation can remain expressed in terms of the convenient system provided the following identity is used to correctly determine the derivative relative to a non-rotating system.

$$\left(\frac{dA}{dt}\right)_{XYZ} = \left(\frac{dA}{dt}\right)_{xyz} + \Omega \times A \quad (2)$$

where  $A$  is a general vector,  $\Omega$  is the angular velocity of the rotating  $xyz$  system relative to the non-rotating  $XYZ$  system, and  $\left(\frac{dA}{dt}\right)_{xyz}$  is the time derivative of the vector as inferred by an observer located on the rotating  $xyz$  system. With that identity, Euler's equation becomes:

$$M_{cm} = \left(\frac{dH_{cm}}{dt}\right)_{xyz} + \Omega \times H_{cm} \quad (3)$$

The task at hand is to define the relationship of the convenient coordinate system to the non-rotating coordinate system. This is often accomplished by defining a sequential set of rotations of the convenient system about one axis at a time, beginning with the convenient system aligned with the non-rotating system. These rotations are referred to as Euler Angles.

The most convenient system for this problem is a simplification of the standard way that body rotations are described for aircraft.<sup>4</sup> The axis of symmetry of the aircraft is first aligned with the  $X$  axis of a system that maintains its origin at the center of mass of the aircraft, but does not rotate. The  $X$  axis is horizontal pointing forward, the  $Y$  axis points to the right of the aircraft, and the  $Z$  axis points down. This is shown in Figure 2. For purposes of this study, the velocity stays aligned with the  $X$  axis. The first rotation is a positive rotation about the  $Z$  axis an angle  $\psi$ , which results in a new  $X$  and  $Y$  axis position, next is a rotation about the new  $Y$  axis an angle  $\theta$ . A full, body-fixed axis system would now incorporate any roll about the new  $X$  axis in a roll angle  $\phi$ . Since the REFS missile spins at a substantial rate about the new  $X$  axis, and since the missile is assumed

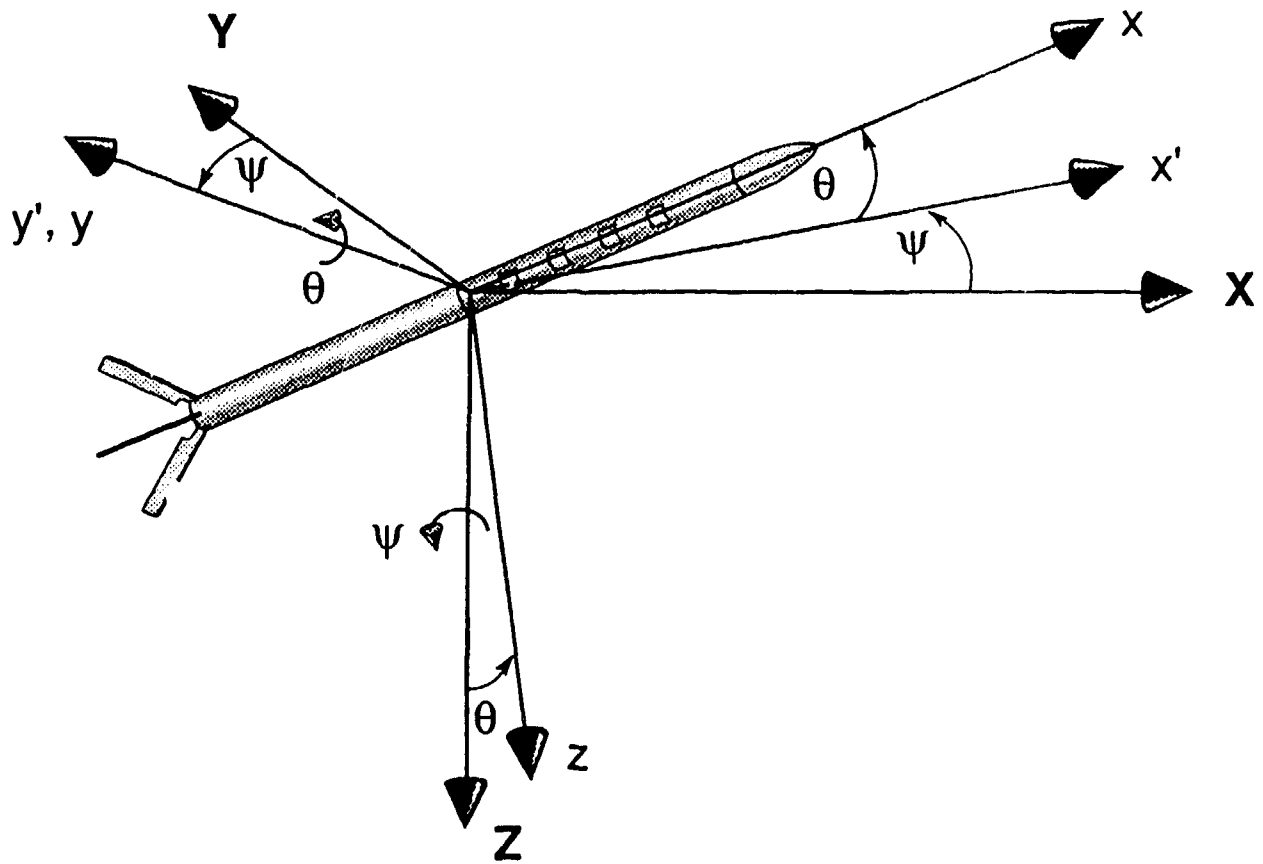


Figure 2: The Yaw-Pitch Euler Angle Coordinate System

to experience forces and moments that are independent of the roll position, the coordinate system for this study will not go through this final rotation. The convenient  $xyz$  system has the  $x$  axis aligned with the axis of symmetry of the missile pointing forward, the  $y$  axis always remains in the horizontal plane toward the right when looking at the missile from the rear, and the  $xz$  plane is always a vertical plane, with the  $z$  axis orthogonal to the  $x$  and  $y$  axes. Due to symmetry, the  $xyz$  system is a principal axis system with no cross moments of inertia and with  $I_{yy}$  equal to  $I_{zz}$ , which will be referred to as  $I'$ .  $I_{xx}$  will be referred to as simply  $I$ .

The components of the angular velocity vector  $\omega$ , expressed in the convenient system, are expressed as follows: the angular velocity  $p$  about the  $x$  axis,  $q$  about the  $y$  axis, and  $r$  about the  $z$  axis. The angular momentum, in

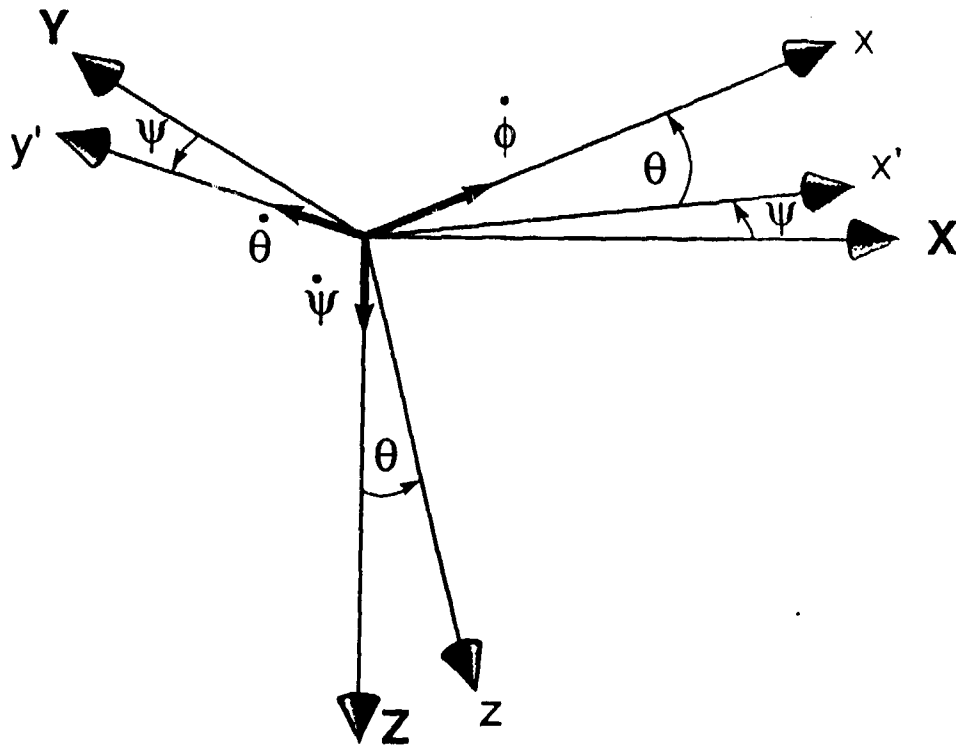


Figure 3: The Angular Velocities in the Yaw-Pitch Euler Angle Coordinate System

the body system coordinates, is simply:

$$\mathbf{H}_{cm} = I p \mathbf{i} + I' q \mathbf{j} + I' r \mathbf{k} \quad (4)$$

where  $\mathbf{i}$ ,  $\mathbf{j}$ , and  $\mathbf{k}$  are unit vectors in the  $xyz$  system. Note that the spinning outer shell of the payload section could affect the overall angular momentum of the vehicle, but for this missile it has a negligible contribution and has been ignored. The angular velocity must also be expressed in terms of the angular velocities of the Euler angles. By inspection of Figure 3, it can be seen that the body-fixed rates are related to the Euler angle rates by the equations:

$$\begin{aligned} \omega_x = p &= \dot{\phi} - \dot{\psi} \sin \theta \\ \omega_y = q &= \dot{\theta} \\ \omega_z = r &= \dot{\psi} \cos \theta \end{aligned} \quad (5)$$

The angular momentum of the missile, expressed in terms of the Euler angles, is:

$$\mathbf{H}_{cm} = I (\dot{\phi} - \dot{\psi} \sin \theta) \mathbf{i} + I' \dot{\theta} \mathbf{j} + I' \dot{\psi} \cos \theta \mathbf{k} \quad (6)$$

Since the  $x$  axis always points to the nose, the moments of inertia in this system are independent of the rotations. The time derivative of  $\mathbf{H}$  as inferred by an observer on the  $xyz$  system is then:

$$\begin{aligned} \left( \frac{d\mathbf{H}_{cm}}{dt} \right)_{xyz} &= I (\ddot{\phi} - \ddot{\psi} \sin \theta - \dot{\psi} \dot{\theta} \cos \theta) \mathbf{i} \\ &+ I' \ddot{\theta} \mathbf{j} + I' (\ddot{\psi} \cos \theta - \dot{\psi} \dot{\theta} \sin \theta) \mathbf{k} \end{aligned} \quad (7)$$

The rotation of the  $xyz$  coordinate system is the same as the rotation of the missile except for the final  $\phi$  about the  $x$  axis:

$$\boldsymbol{\Omega} = -\dot{\psi} \sin \theta \mathbf{i} + \dot{\theta} \mathbf{j} + \dot{\psi} \cos \theta \mathbf{k} \quad (8)$$

When the cross product and the time derivative are substituted back into Euler's Equation, the following scalar equations result:

$$\begin{aligned} \sum T_x &= I \ddot{\phi} - I \ddot{\psi} \sin \theta - I \dot{\psi} \dot{\theta} \cos \theta \\ \sum T_y &= I' \ddot{\theta} + (I' - I) \dot{\psi}^2 \sin \theta \cos \theta + I \dot{\psi} \dot{\phi} \cos \theta \\ \sum T_z &= I' \ddot{\psi} \cos \theta - (2I' - I) \dot{\psi} \dot{\theta} \sin \theta - I \dot{\theta} \dot{\phi} \end{aligned} \quad (9)$$

The above procedures yield equations of rotational motion with all the kinematic terms as functions of the Euler angles and with moments computed relative to the convenient body pointing, but not fully body fixed, coordinates. The aerodynamic forces and moments are defined and most easily expressed in terms of these body pointing coordinates. To have a complete set of equations for solution, equations relating position relative to the body pointing system to the Euler angle system must be developed. These are obtained by determining the direction of the velocity vector in both systems. Since, for this work, the velocity vector is always aligned with  $X$ , the components of velocity relative to the body system are simple functions of the Euler angles. The velocity vector in terms of the fixed system is:

$$\mathbf{V} = V \mathbf{I} + 0 \mathbf{J} + 0 \mathbf{K} \quad (10)$$

To obtain the components in terms of the new basis vectors of the body system, the components in the original system are left multiplied by the two rotation matrixes that describe first a positive rotation  $\psi$  about the  $Z$  axis followed by a positive rotation  $\theta$  about the new  $Y$  axis<sup>3</sup> as follows:

$$\begin{bmatrix} u \\ v \\ w \end{bmatrix} = \begin{bmatrix} \cos \theta & 0 & -\sin \theta \\ 0 & 1 & 0 \\ \sin \theta & 0 & \cos \theta \end{bmatrix} \begin{bmatrix} \cos \psi & \sin \psi & 0 \\ -\sin \psi & \cos \psi & 0 \\ 0 & 0 & 1 \end{bmatrix} \begin{bmatrix} V \\ 0 \\ 0 \end{bmatrix} \quad (11)$$

This results in the three components:

$$\begin{aligned} u &= V \cos \theta \cos \psi \\ v &= -V \sin \psi \\ w &= V \sin \theta \cos \psi \end{aligned} \quad (12)$$

The position of the body relative to the velocity vector is expressed in terms of the angle of attack,  $\alpha$ , and the angle of sideslip,  $\beta$ . A useful angle is the "total angle of attack",  $\Theta$ , a single angle incorporating the effect of both angle of attack and angle of sideslip. These angles can be expressed in terms of the Euler angles by applying the definitions:

$$\begin{aligned} \tan \alpha &= w/u \\ \sin \beta &= v/V \\ \cos \Theta &= u/V \end{aligned} \quad (13)$$

when the components from Eq. 12 are substituted into the above, the following identities result:

$$\begin{aligned} \alpha &= \theta \\ \beta &= -\psi \\ \Theta &= \cos^{-1}(\cos \theta \cos \psi) \end{aligned} \quad (14)$$

For the sake of completeness, it is useful here to develop the angle of attack and sideslip relationships relative to a complete body fixed coordinate system. The output of 6DOF simulations is usually in terms of these angles, which are subscripted with  $BF$  in this work to distinguish them from the body pointing system. In order to express the velocity vector in a full body fixed system, one more rotation must be accomplished: a rotation of a positive angle  $\phi$  about the new X axis. This is accomplished by the matrix operation:

$$\begin{bmatrix} u_{BF} \\ v_{BF} \\ w_{BF} \end{bmatrix} = \begin{bmatrix} 1 & 0 & 0 \\ 0 & \cos \phi & \sin \phi \\ 0 & -\sin \phi & \cos \phi \end{bmatrix} \begin{bmatrix} V \cos \theta \cos \psi \\ -V \sin \psi \\ V \sin \theta \cos \psi \end{bmatrix} \quad (15)$$

This results in the following equations for the velocity components:

$$\begin{aligned} u_{BF} &= V \cos \theta \cos \psi \\ v_{BF} &= -V \cos \phi \sin \psi + V \sin \phi \sin \theta \cos \psi \\ w_{BF} &= V \sin \phi \sin \psi + V \cos \phi \sin \theta \cos \psi \end{aligned} \quad (16)$$

Now apply the definitions of the angles in Eq. 13 to obtain:

$$\begin{aligned} \alpha_{BF} &= \tan^{-1}(\sin \phi \tan \psi \sec \theta + \cos \phi \tan \theta) \\ \beta_{BF} &= \sin^{-1}(-\cos \phi \sin \psi + \sin \phi \sin \theta \cos \psi) \end{aligned} \quad (17)$$

These are usually simplified by making the small angle assumptions for the angles  $\psi$ ,  $\theta$ ,  $\alpha_{BF}$ , and  $\beta_{BF}$ . The total angle of attack is the same in either coordinate system.

## 2.2 The Moments

### 2.2.1 Roll Moments:

The FFAR configuration that was used for this project has four exhaust nozzles. Each nozzle is "scarfed," that is, truncated by a plane that is not normal to the nozzle centerline. This results in a tangential component to the thrust. The nozzles are scarfed in a direction that results in the side thrust being perpendicular to the centerline of the missile. The magnitude of the moment of these canted nozzle sets is not contained in any of the known documentation. The value of the roll moment and the roll moment coefficients used in this analysis were deduced from rotation data acquired by William P. Winn.<sup>5</sup> The roll moments considered for the simulation are the moment due to thrust,  $L_T$ , and roll damping,  $L_p$ . When substituted into a simple, one dimensional roll rotation equation, the result is:

$$\dot{p} = (L_T + L_p)/I \quad (18)$$

The roll damping moment, expressed in terms of the non-dimensional roll damping coefficient, is:

$$L_p = \left(\frac{\lambda^2 S}{2}\right)\left(\frac{\rho V}{2}\right) C_{lp} p \quad (19)$$

where:

- $C_{lp}$  = The roll damping coefficient (n.d.)
- $S$  = Reference Area (missile cross sectional area) (ft<sup>2</sup>)
- $\lambda$  = Reference Length (missile diameter) (ft)
- $\rho$  = Air density (slugs/ft<sup>3</sup>)

Winn's data showed a roll velocity increase from about 1 rev/s at the exit of the launch tube to about 24 revs/s at burnout, then what appeared to be an exponential decay. A  $C_{lp}$  value of -0.25 produced an initial roll decay rate that matched Winn's data after burnout. Then with this roll damping, the rocket thrust moment in the roll direction was determined that produced the observed spinup. The resulting moment was 0.349 ft-lbs at the full thrust of 734 lb. This represents a thrust offset of less than one-half degree with the momentum arm of each nozzle approximately 0.75 in. from the center line. A comparison of the roll simulation to Winn's data is shown in Figure 4.

### 2.2.2 Pitch and Yaw Moments:

Except for the moments resulting from the Magnus Effect, the moments used in this analysis are standard for aircraft and missile analysis. Therefore, these will be treated only briefly. Since the vehicle is symmetrical, the coefficients

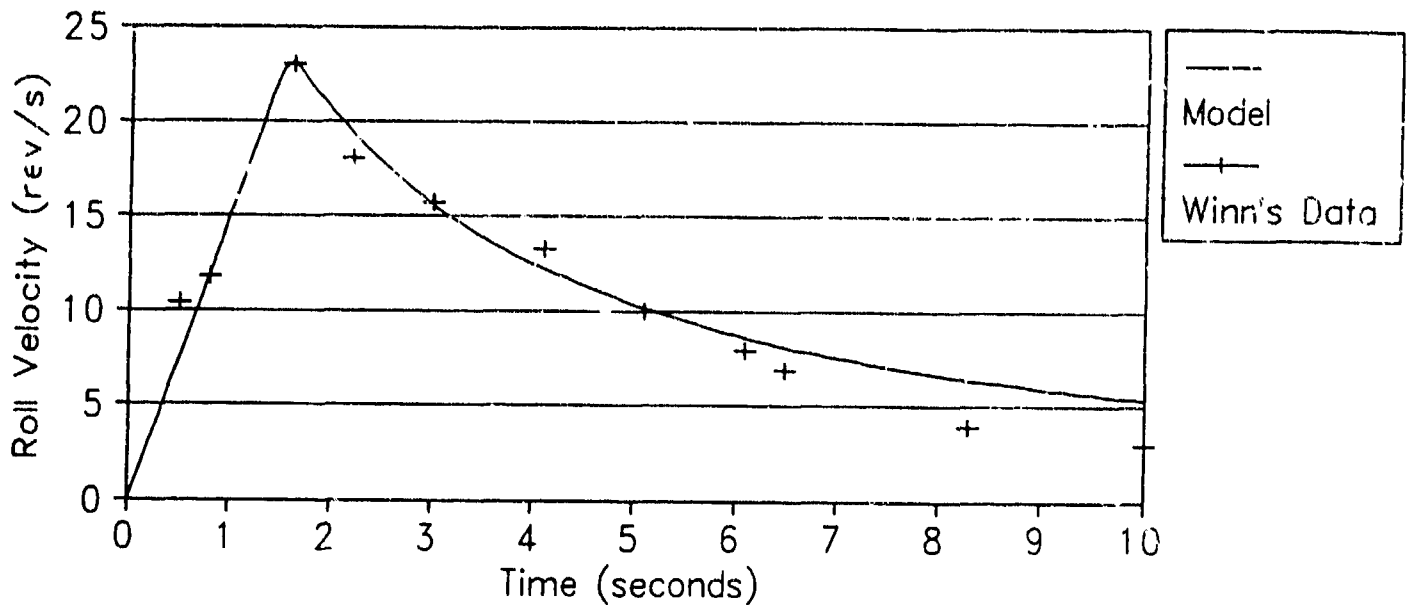


Figure 4: Predicted Roll Output Compared to the Data of Winn

that apply to an angle or angular velocity in the pitch axis are the same as those that apply for the yaw axis. The following discussion will be limited to the aerodynamic forces and moments for the pitch axis. These must be applied in a similar manner to the yaw axis as well. Most of the values for the coefficients were obtained from the USAF Missile DATCOM computer program.<sup>6</sup> This program is a special adaptation of the USAF Stability and Control DATCOM methodology<sup>7</sup> for missile shapes.

The primary pitching moment is the result of the sum of all of the inplane forces that results when a vehicle is at an angle of attack to the velocity vector. Using the "linear aerodynamics" assumption, the normal force,  $N_\alpha$  is computed as follows:

$$N_\alpha = C_{N_\alpha} Q S \alpha \quad (20)$$

where:

$C_{N_\alpha}$  = The normal force coefficient (n.d.)  
 $Q$  =  $\frac{1}{2} \rho V^2$ , the dynamic pressure (lb/ft<sup>2</sup>)

Care must be taken since the coefficient is often expressed either per degree or per radian of pitch angle. This coefficient is the result of the contributions from all the aerodynamic surfaces of the vehicle, which are computed separately. The full vehicle coefficient is not a straight sum of each of the

individual effects since the presence of other parts of the body will modify the contribution of the individual surface. In this case, the parts of the vehicle are the body and the fins. There does not seem to be much interference since the total effect is approximately equal to the sum of  $C_{N\alpha \text{ fins}}$  and  $C_{N\alpha \text{ body}}$ . The fin contribution is between 50 and 60 percent of the total. The DATCOM  $C_{N\alpha}$  values were entered into the analysis as a tabular function of mach number, and  $C_{N\alpha \text{ fins}}$  was estimated to be a constant 60 percent of  $C_{N\alpha}$ . Required values are determined by interpolation of the data.

The pitching moment on the vehicle,  $M_\alpha$  is computed in terms of the non-dimensional pitching moment coefficient as follows:

$$M_\alpha = C_{m\alpha} Q S \lambda \alpha \quad (21)$$

The moment about the center of mass of the normal forces on the vehicle can be collectively expressed as a single total normal force acting at a point called the center of pressure,  $X_{cp}$ . This is a function of Mach number and is one of the outputs of the DATCOM program. The DATCOM data is also entered as a table in the 3DOF program. The position of the center of mass,  $X_{cm}$ , has been determined from the actual flight hardware for the time before the missile is fired and the time after the propellant has been expended. It has been assumed that  $X_{cm}$  varies linearly with time from launch to burnout, then stays constant for the remainder of the flight. For this analysis, the aerodynamic pitching moment coefficient is computed as a function of three tabulated functions:

$$C_{m\alpha} = C_{N\alpha} (X_{cp} - X_{cm}) / \lambda \quad (22)$$

This coefficient normally is the basis of the static stability of the vehicle about the pitch axis. If the coefficient is negative, the vehicle is statically stable; that is, if there is a positive angle of attack, the resulting moment will be negative, causing a restoration to zero angle of attack. The sign of the coefficient is negative if the center of pressure is located behind the center of mass (positive  $x$  is in the direction of the front of the vehicle). The difference between the two lengths is a measure of vehicle stability and is known as the static margin, often expressed in multiples of the missile diameter.

There is a moment that results from the rate of change of pitch,  $q$ . Assuming linear aerodynamics, this moment,  $M_q$  is expressed in terms of a non-dimensional coefficient as follows:

$$M_q = C_{mq} \lambda S Q \frac{\lambda q}{2V} \quad (23)$$

The "pitch damping derivative"  $C_{mq}$  can be computed from the  $C_{N\alpha}$  for each component and the distance between  $X_{cp}$  for the component and  $X_{cm}$  for the vehicle. For a missile, the primary contributor to the coefficient is the tail

surface, so the following approximate expression<sup>8</sup> was used for this analysis:

$$C_{mq} = -2C_{N\alpha} \sin\alpha [(X_{cp} \sin\alpha - X_{cm \text{ vehicle}})/\lambda]^2 \quad (24)$$

A second damping moment is jet damping, which can be significant in the very early phase of the flight. Jet damping is the term used to describe the reduction of angular momentum of a body that is losing mass. The formula for jet damping is:

$$M_{JD_i} = -\omega_i \dot{m} (l_{\perp i}^2 - k_i^2) \quad (25)$$

where:

$M_{JD_i}$  = Moment about the  $i^{\text{th}}$  axis

$\omega_i$  = Angular velocity about the  $i^{\text{th}}$  axis

$\dot{m}$  = Jet exhaust mass flow rate

$l_{\perp i}$  = the distance from the center of mass to the nozzle exit, in a direction perpendicular to  $i^{\text{th}}$  direction.

$k_i$  = the radius of gyration about the  $i$  axis =  $\sqrt{I_i/m}$

### 2.2.3 Magnus Moments

The classical analysis of the Magnus effect considers the aerodynamic effects of a spinning cylinder in a cross flow. A potential flow theory analysis, which represents the spinning cylinder by a source/sink couple with circulation, results in the prediction of a normal force (lift) and no drag. As White<sup>9</sup> points out, experiments show that the lift is, at best, only about one-half that predicted, and spinning causes the drag to increase above the value experienced by a non-rotating cylinder. The results are nicely summarized in Figure 5, from White. The theoretical (potential theory) coefficient of lift, using White's nomenclature is:

$$C_L = \frac{L}{Q_{\infty} S} = \frac{2\pi a \omega}{U_{\infty}} \quad (26)$$

where:

$a$  = cylinder radius (ft)

$b$  = cylinder length (ft)

$L$  = Normal force (Lift) (lb)

$Q_{\infty} = \frac{1}{2} \rho U_{\infty}^2$  (lb/ft<sup>2</sup>)

$S = 2 b a$ , the cross sectional area of the cylinder (ft<sup>2</sup>)

$U_{\infty}$  = Cross flow velocity (ft/s)

$\omega$  = angular velocity of cylinder (1/s)

$\rho$  = fluid density (slugs/ft<sup>3</sup>)

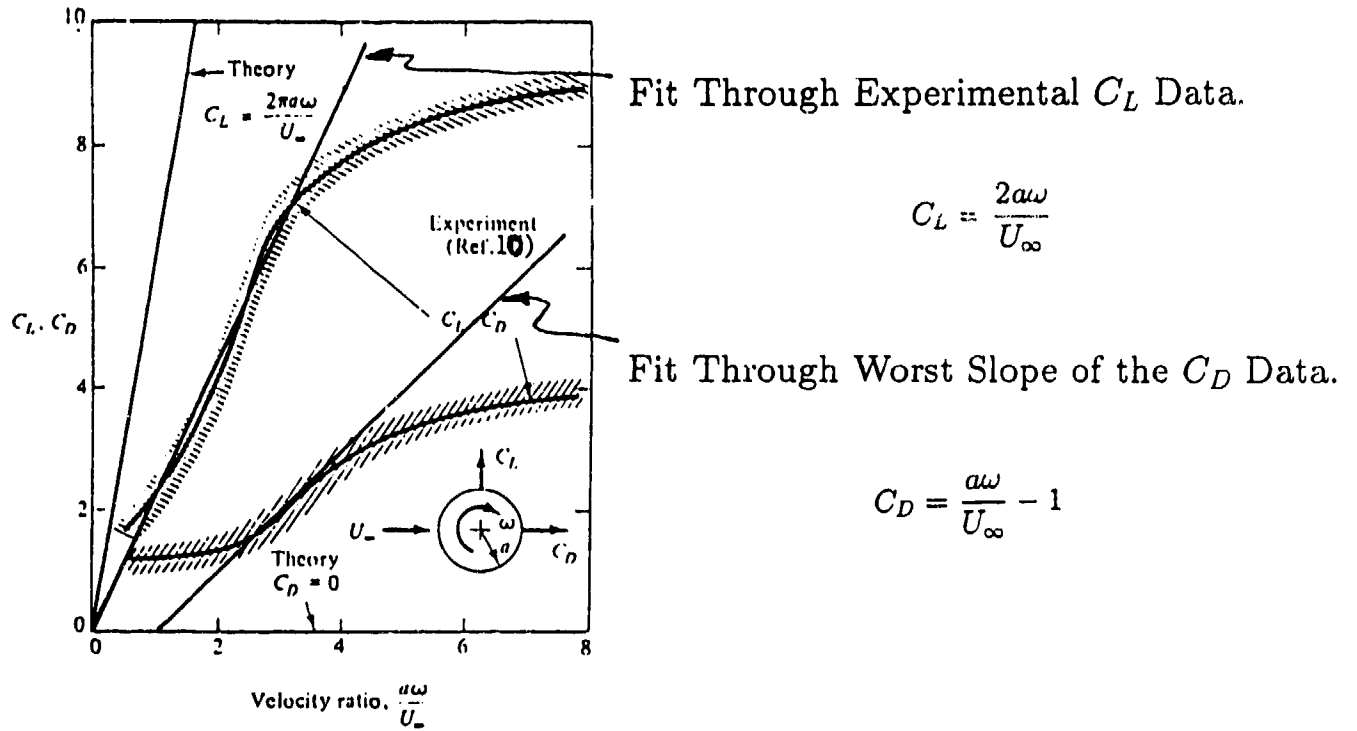


Figure 5: Magnus Lift and Drag Figure from Reference 9, Originally From Reference 5, With the Curve Fits Through the Experimental Data Used for This Study

The experimental values for both drag and lift coefficients tend to approach asymptotic values at high velocity ratios, which means at high rotation rates, the lift and drag are independent of the rotational velocity. Similarly, the experimental coefficient of drag at low rotation rates is independent of rotation rate. In any flat region, the Magnus force for the two parts of the REFS missile would be identical to the result if the entire missile were spinning at the same rate, and the Magnus moments would be no larger than for a typical spinning missile. It is in those regions where the coefficients have the greatest slope that one would experience the greatest difference in force for the two spinning sections, and, hence, the greatest Magnus moments. Since this analysis is only an approximate attempt to determine the worst case Magnus effect, the coefficients will be assumed to follow a linear relationship to velocity ratio, using the value through the regions of greatest slope. Two additional lines are shown on the curve. The equations of these lines are:

$$C_L = \frac{2a\omega}{U_\infty} \quad (27)$$

$$C_D = \frac{a\omega}{U_\infty} - 1 \quad (28)$$

The approximate Magnus results are now applied to the dual spinning cylinders of the REFS missile. Two views of the missile are shown in Figure 6. The view on the lower left is an elevation view that is normal to the pitch plane and shows the missile at a total angle of attack  $\alpha$  to the free stream velocity vector  $V$ . It is assumed that  $U_\infty$  for the Magnus calculation is the cross wind component of  $V$ , or  $V \sin \alpha$ , which is customary for projectile analysis. It is further assumed that the Magnus force for each section of the cylinder is not influenced by the spinning of the other section. One could imagine that the swirl induced by the front might modify the flow over the back, but that has been ignored here. The projected view on the upper right is a view from a location in the pitch plane looking in the negative  $z$  direction. From this location, the velocity vector is below the missile, and the cross flow velocity is pointing out of the page. Assuming positive angular velocity  $p$  of the rocket motor (the rear section) and a positive increment of angular velocity  $\Delta p$  of the front cylinder, then both Magnus lift vectors point toward the left, or the negative  $y$  direction, and the lift on the front is larger than that of the rear. On this side of the missile, the tangential velocity due to rotation is in the same direction as the cross flow velocity. Using the subscript 1 to denote the front cylinder of the missile and 2 to denote the rear cylinder, the magnitude of the lift on the second cylinder is:

$$L_2 = (C_L)_2 Q_\infty 2 b_2 a_2 \quad (29)$$

$$L_2 = \left( \frac{2ap}{U_\infty} \right) \left( \frac{\rho U_\infty^2}{2} \right) 2 b_2 a_2 \quad (30)$$

$$L_2 = \rho V \sin \alpha 2 a_2^2 b_2 p \quad (31)$$

Similarly, the lift on the front of the cylinder is:

$$L_1 = \rho V \sin \alpha 2 a_1^2 b_1 (p + \Delta p) \quad (32)$$

The moment caused by these parallel forces has a magnitude about the cm equal to the sum of the product of each force times its moment arm,  $l_i$ . The direction of the moment is out of the page, which is the negative  $z$  direction. Therefore, the vector expression for the moment is:

$$\mathbf{T}_{magL} = -(L_1 l_1 - L_2 l_2) \mathbf{k} \quad (33)$$

In the spirit of the approximate nature of this analysis, the following simplifying assumptions are made: the force center (center of pressure) of each Magnus force is the center of each cylinder, the cylinders have the same radius,  $a$ , and the cylinders are each the same length,  $b$ . Further, it is assumed that the cm is approximately at the joint of the two cylinders, which makes each moment arm  $b/2$ . When applied, the resulting expression for the moment is:

$$\mathbf{T}_{magL} = -\rho V a^2 b^2 (\Delta p) \sin \alpha \mathbf{k} \quad (34)$$

Note that the moment is no longer a function of the rocket motor angular velocity, only the difference between the rotational speeds.

The Magnus drag forces are also shown in Figure 6 in the elevation view. Note that if both  $p$  and  $\Delta p$  are positive, and if we are in a region of increasing  $C_D$ , the drag in the front will be larger than that in the back, causing the resulting moment to be into the page, which is in the positive  $y$  direction. If the above assumptions are applied to the "worst case" linear portion of the drag curve, the result is:

$$\mathbf{T}_{magD} = \frac{1}{2} \rho V a^2 b^2 (\Delta p) \sin \alpha \mathbf{j} \quad (35)$$

The moment from the drag has a magnitude of one-half of that from the lift, and is potentially destabilizing since an increase in  $\alpha$  results in a higher value of the moment that is trying to increase  $\alpha$ . This is resisted by the inherent aerodynamic static stability of the missile provided by the fins, so the magnitudes of each must be examined to determine the stability.

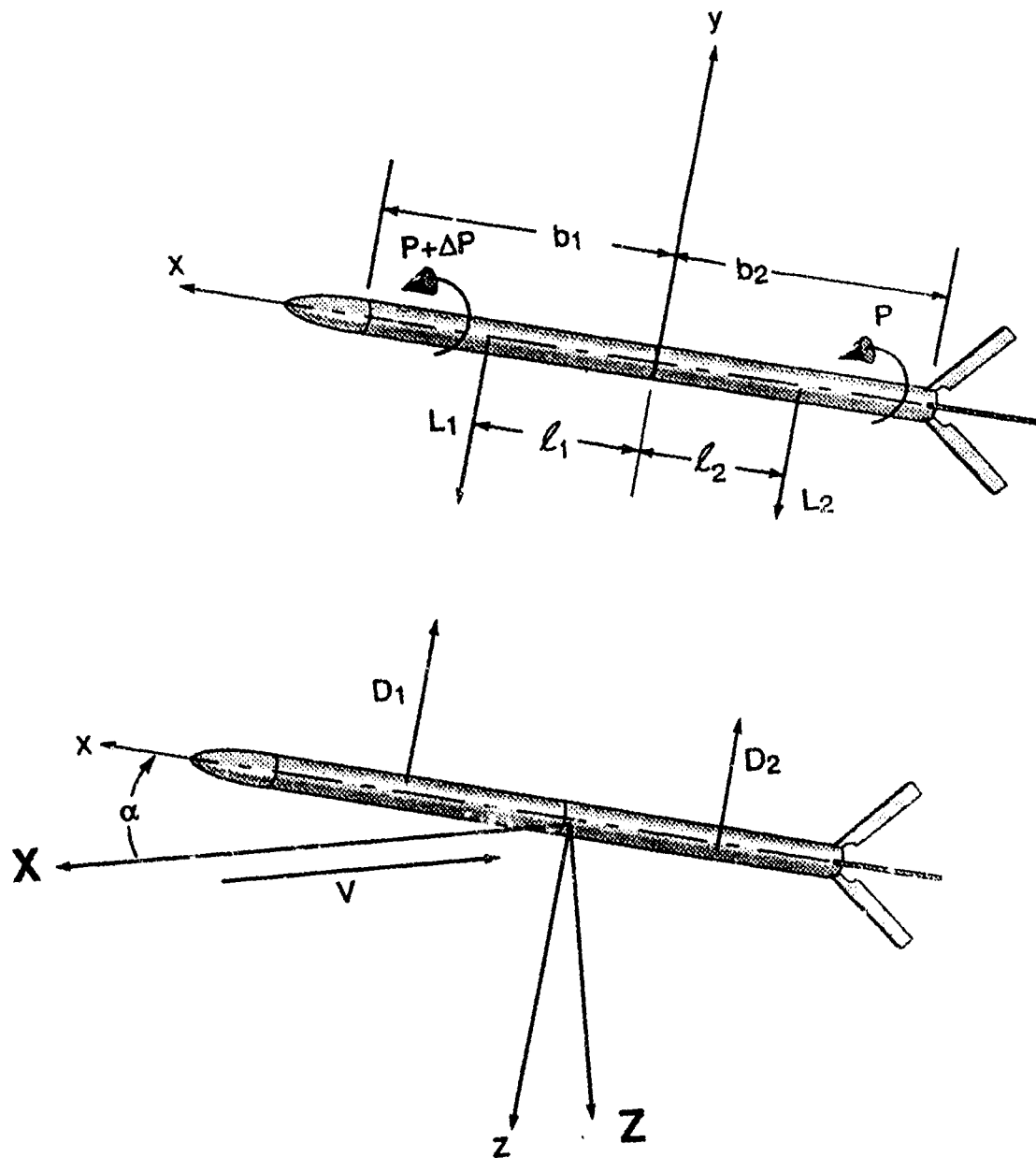


Figure 6: Elevation View of the Pitch Plane and Normal View in the Pitch Plane of the REFS Missile Showing Magnus Lift and Drag Forces

### 2.3 Solution of Equations of Rotation

The aerodynamic moments discussed above are explicit functions of the angle of attack and sideslip and their angular velocities. These can be converted into the euler angles and the euler angular velocities through Eq. 5 and the angle of attack and sideslip conversions mentioned in the descriptions of the coordinate systems. The result is a system of three coupled, non-linear, non-homogeneous, second order ordinary differential equations, with non-constant coefficients. While the equations yield analytical solutions for only some special simplifications, they can be solved easily with numerical methods. Observe that  $\ddot{\theta}$  and  $\ddot{\psi}$  are the only second derivatives in the  $y$  and  $z$  component equations. The value of  $\ddot{\psi}$  can then be substituted into the  $x$  component equation to arrive at an  $x$  component equation with  $\ddot{\phi}$  as the only second derivative.

$$\begin{aligned}\ddot{\phi} &= (\sum T_x + I\ddot{\psi} \sin \theta + I\dot{\psi}\dot{\theta} \cos \theta)/I \\ \ddot{\theta} &= (\sum T_y - (I' - I)\dot{\psi}^2 \sin \theta \cos \theta - I\dot{\psi}\dot{\phi} \cos \theta)/I' \\ \ddot{\psi} &= (\sum T_z + (2I' - I)\dot{\psi}\dot{\theta} \sin \theta + I\dot{\theta}\dot{\phi})/I' \cos \theta\end{aligned}\quad (36)$$

Notice that the third equation is undefined if  $\theta$  goes to 90 degrees. This should not be a problem for a well behaved missile, since this angle is the angle of attack. In practice, these equations are treated as three first order equations in the angular velocities, and three additional first order equations for the angles complete the equation set:

$$\begin{aligned}\dot{\phi} &= \int_0^T \ddot{\phi} dt + \dot{\phi}_0 \\ \dot{\theta} &= \int_0^T \ddot{\theta} dt + \dot{\theta}_0 \\ \dot{\psi} &= \int_0^T \ddot{\psi} dt + \dot{\psi}_0 \\ \phi &= \int_0^T \dot{\phi} dt + \phi_0 \\ \theta &= \int_0^T \dot{\theta} dt + \theta_0 \\ \psi &= \int_0^T \dot{\psi} dt + \psi_0\end{aligned}\quad (37)$$

The initial positions of the angles and angular velocities are all that is required to start the solution. The strategy for this analysis was to provide a slight perturbation at the beginning and observe the progress of the solution. The perturbation was to set the initial angle of attack,  $\theta_0$ , equal to 5 degrees, the roll velocity,  $\dot{\psi}_0$  is set to 1 revolution per second, and all of the other angles and angular velocities equal to 0. As the solution progressed, if the angle of attack tended to increase, the missile was deemed unstable. If the angle of attack tended towards 0, the missile was deemed stable.

Parameter	Value
$a$	0.1163 ft
$b$	3.0 ft
$C_{lp}$	-0.25
$C_{Na}$	7.99 to 16.87 per radian
$I_x$	0.00496 to 0.00363 slug-ft <sup>2</sup>
$I_y$ and $I_z$	2.146 to 1.514 slug-ft <sup>2</sup>
$L_T$	0.349 ft-lbs
Mass	0.7736 to 0.5774 slugs
$\dot{m}$	0.1266 slugs/s
$S$	0.04246 ft <sup>2</sup>
$V$	0 to 2400 ft/s
$X_{cm}$	41.9 to 35.9 in from nose
$X_{cp}$	52.8 to 69.1 in from nose
$\Delta P$	-15 rev/s and +15 rev/s
$\lambda$	0.2325 ft

Table 1: Parameters for REFS System Analysis

### 3 RESULTS

The principal result of this analysis is that the REFS missile configuration is very stable. The conditions for the analysis are listed in Table 1. The inherent static stability from the fins is well in excess of that required to overcome the moments from Magnus lift and drag. Figures 7 and 8 show the moments about the pitch axis with positive and negative forward section spin respectively. In both cases, the Aero Restoring moment (from  $C_{m\alpha}$ ) gets larger than 30 ft-lbs while the Magnus moments are on the order of less than 0.5 ft-lb. Note that the Aero Damping moment (from  $C_{mq}$ ) and the jet damping moments are the second and third largest moments. The pitch plane moment from Magnus lift is lower than from Magnus drag in apparent contradiction to what is expected from the coefficients. Pitch plane moment from Magnus lift is the result of angle of sideslip. Since the initial condition is an angle of attack only, sideslip angle is never very large compared to the angle of attack, so the resulting moments are much lower.

The effect on total angle of attack is shown in Figure 9. In these plots, angle of attack is shown for the DATCOM predicted  $C_{m\alpha}$ , for one-half that value, and for one-tenth of that value. In every case the missile is stable, although the positive spin case with the lowest coefficient is noticeably slower in damping the disturbance.

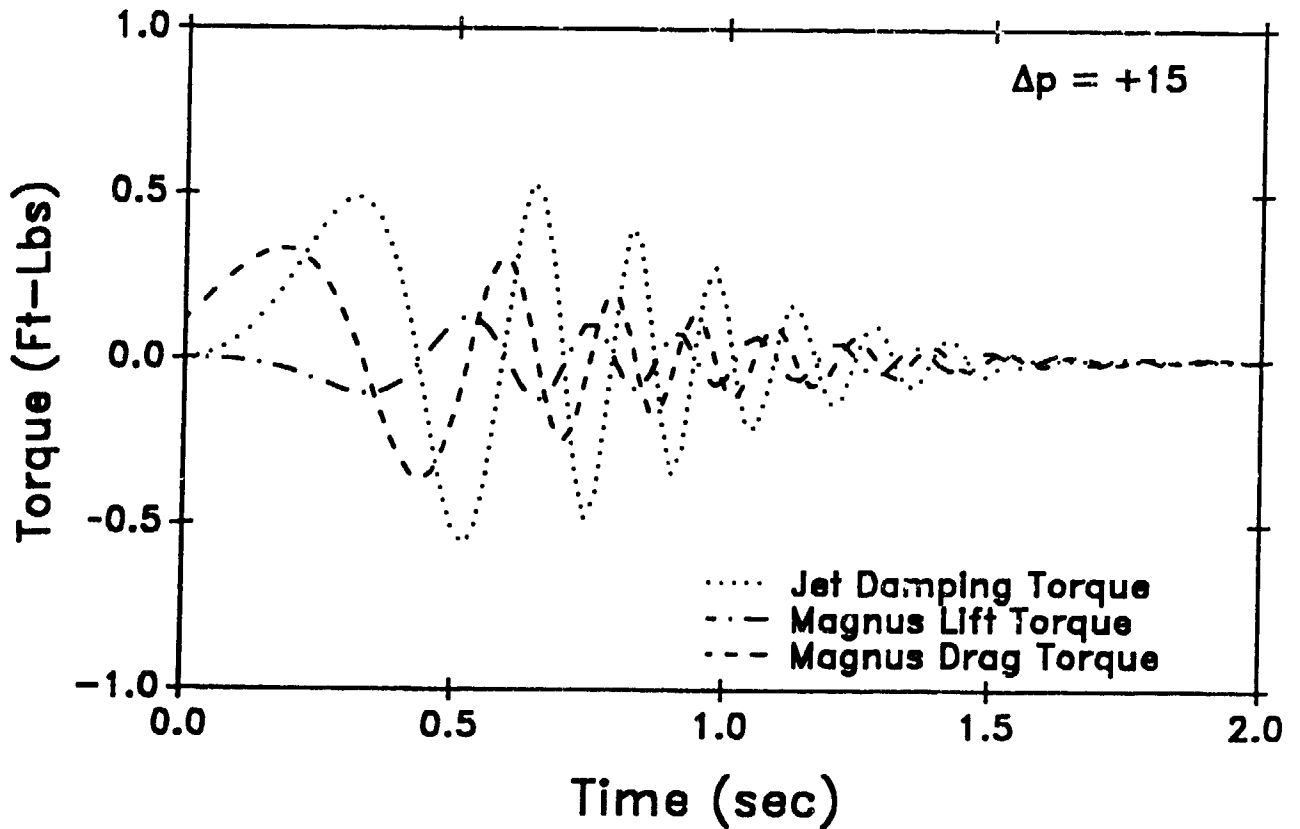
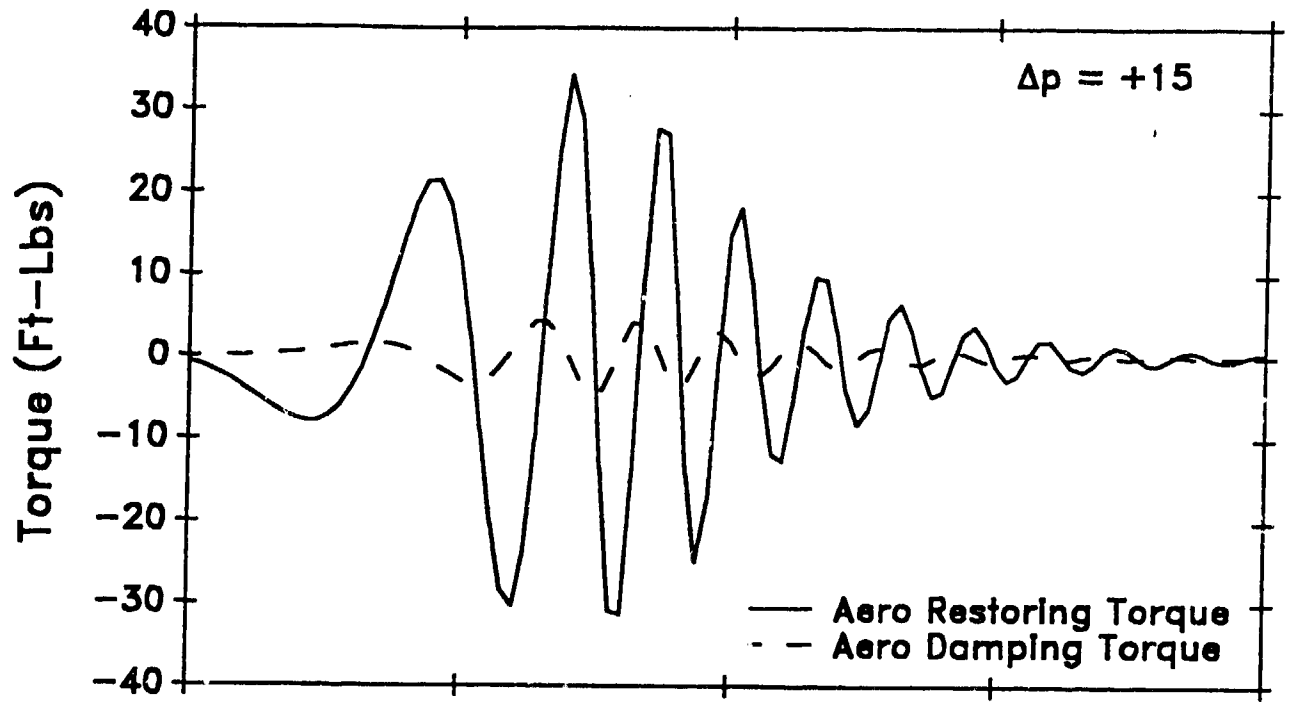


Figure 7: Pitch Plane Moments on the REFS Missile With Positive Forward Section Rotation as a Function of Time

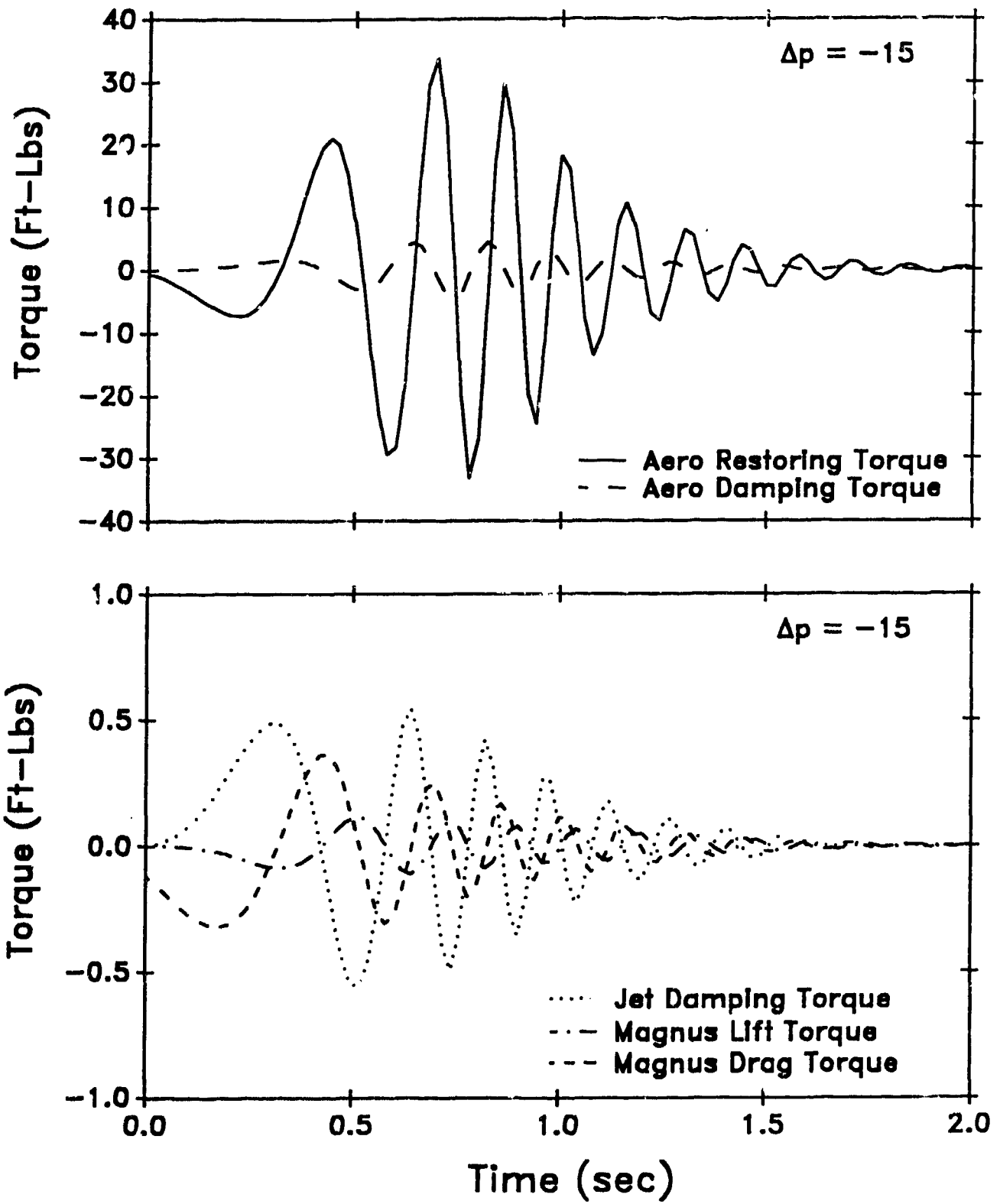


Figure 8: Pitch Plane Moments on the REFS Missile With Negative Forward Section Rotation as a Function of Time

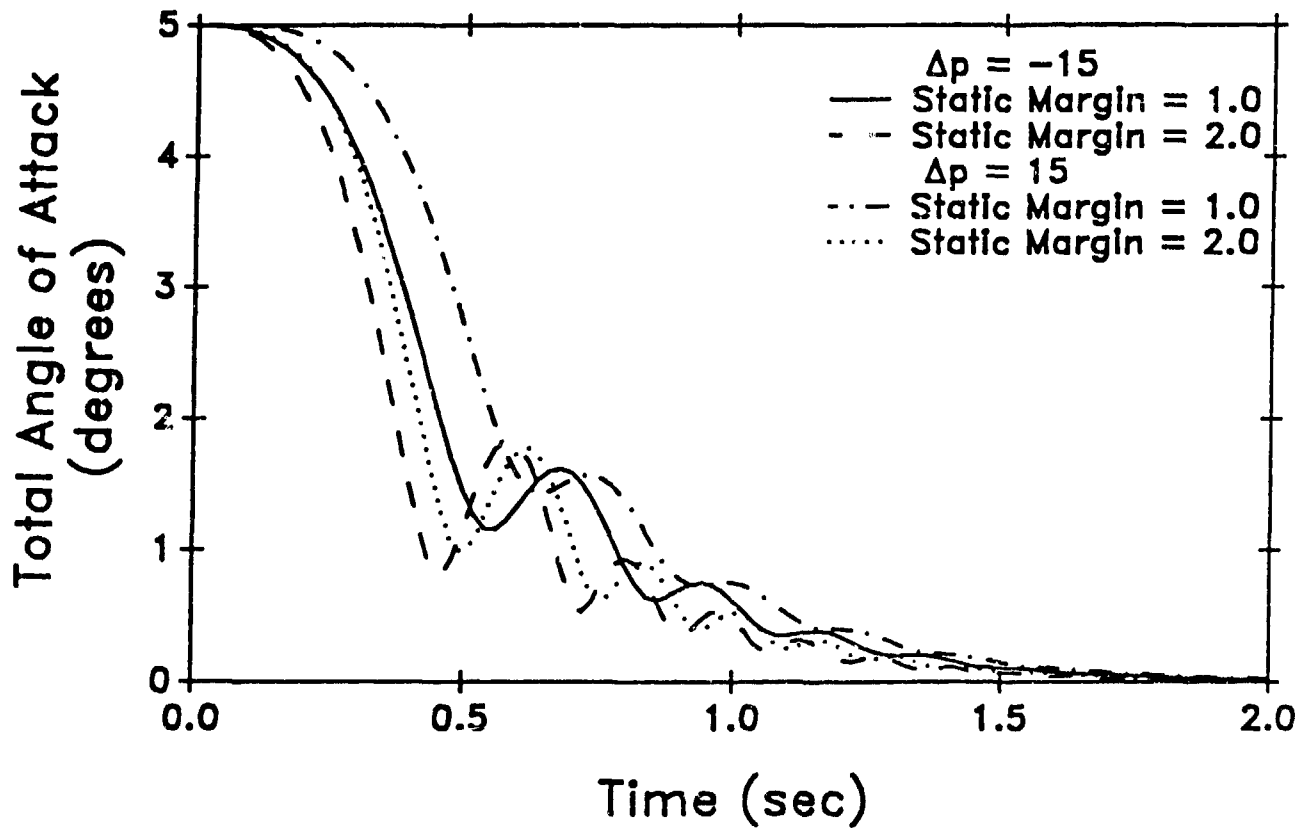


Figure 9: Total Angle of Attack Versus Time With Positive and Negative Forward Section Rotation

As mentioned above, the REFS missile static margin is high. The static margin is in excess of 5 missile diameters, while 1 to 2 diameters is more typical. Figure 10 shows the total angle of attack versus time with the more typical static margins of 1 and 2 diameters. These margins appear sufficient to overcome any Magnus moments.

An interesting result of this analysis is that the effects of the Magnus moments are slightly less severe when the front section is spun in the negative direction. This is especially evident in Figure 10, which shows both forward spin directions on the same plot.

Finally, the one clear effect of front section spin is in the direction of precession taken by the missile as the nose converges to the center. Notice in Equation 34 that, given a positive angle of attack and no sideslip, the sign of the moment about the  $z$  axis is the negative of the sign of the forward spin. Therefore, a positive  $\Delta p$  results in an initial tendency for negative  $z$  moment resulting in an initially negative tendency in  $\phi$ , which is a positive sideslip angle  $\beta$ . So, when viewed from the rear, the nose of the REFS experiment would precess in a counterclockwise direction with positive  $\Delta p$  and would precess in a clockwise direction with negative  $\Delta p$ . This is demonstrated in the plots in which the Euler angle  $\theta$  is shown as a function of the Euler angle  $\psi$  (Figure 11).

#### Stability Considerations:

The results of the above analysis invite a more fundamental look at the problem to determine when the Magnus effects could cause a disturbance to missile flight.

**The Bank - Pitch Coordinate System:** The Yaw-Pitch Coordinate system was used to analyze the angular motion of the REFS missile. There is another coordinate system that is convenient for stability arguments and for visualization of the moments on the missile. That is the "Bank - Pitch" system, which is often used to analyze the motion of a top or gyroscope.<sup>3</sup> As shown in Figure 12, this system begins with a rotation an angle  $\psi$  about the  $X$  axis, followed by a rotation of  $\theta$  about the new  $Y$  axis. Again, the missile is allowed to rotate an angle  $\phi$  about the new  $X$  axis, but the coordinate system does not perform this final rotation. In top or gyroscopic motion, the angle  $\theta$  is referred to as the nutation angle and  $\psi$  is called the precession angle.

If the new angular definitions are applied to the Euler equations in a manner similar to the initial part of this report, the following scalar equations of rotational motion result:

$$\begin{aligned}
 \sum T_x &= I\ddot{\phi} + I\dot{\psi}\cos\theta - I\dot{\psi}\dot{\theta}\sin\theta \\
 \sum T_y &= I'\ddot{\theta} - (I' - I)\dot{\psi}^2\sin\theta\cos\theta + I\dot{\psi}\dot{\phi}\sin\theta \\
 \sum T_z &= I'\dot{\psi}\sin\theta + (2I' - I)\dot{\psi}\dot{\theta}\cos\theta - I\dot{\theta}\dot{\phi}
 \end{aligned}
 \tag{38}$$

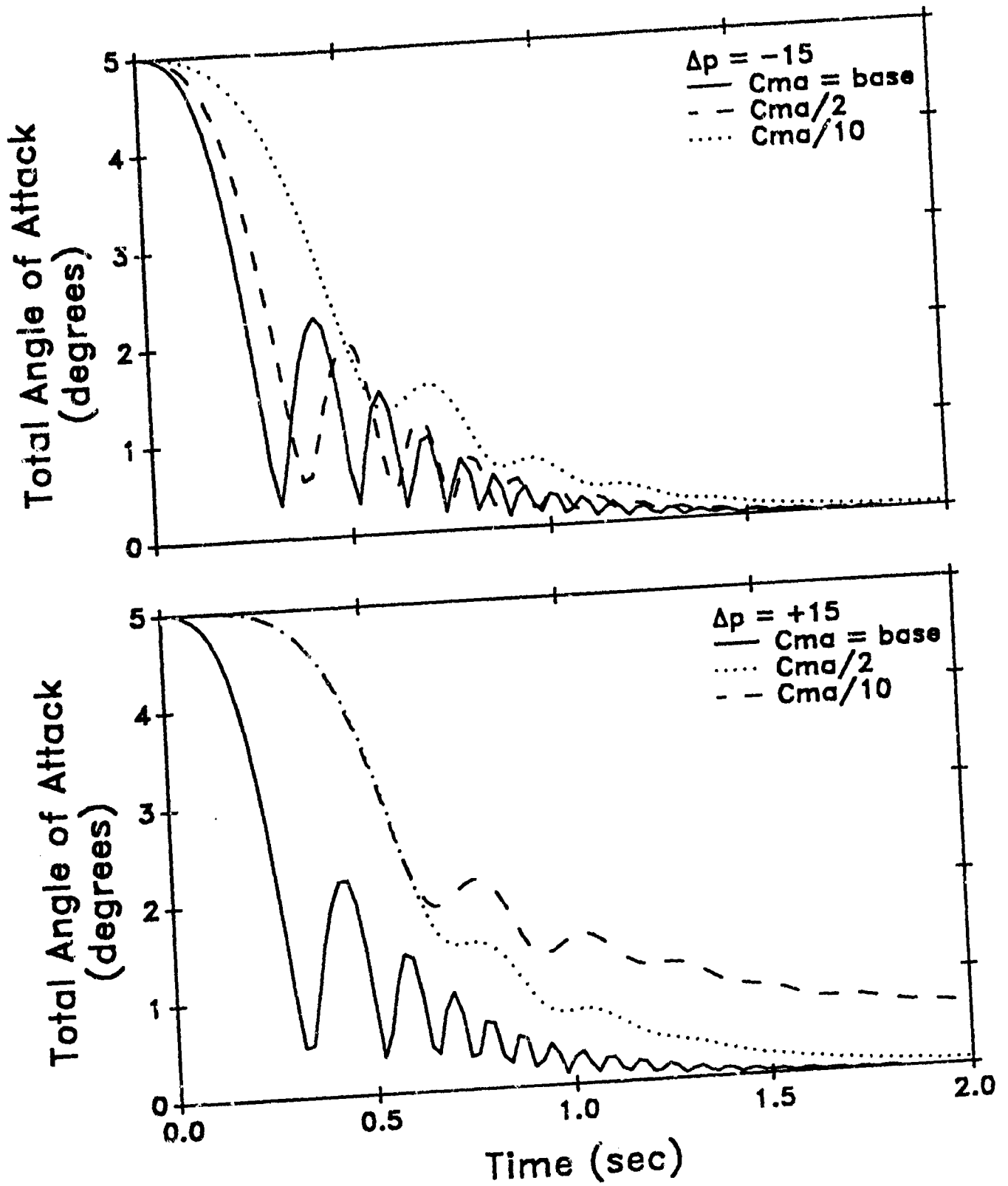


Figure 10: Total Angle of Attack for Two Values of Static Margin for Both Positive and Negative Angle Forward Section Rotation

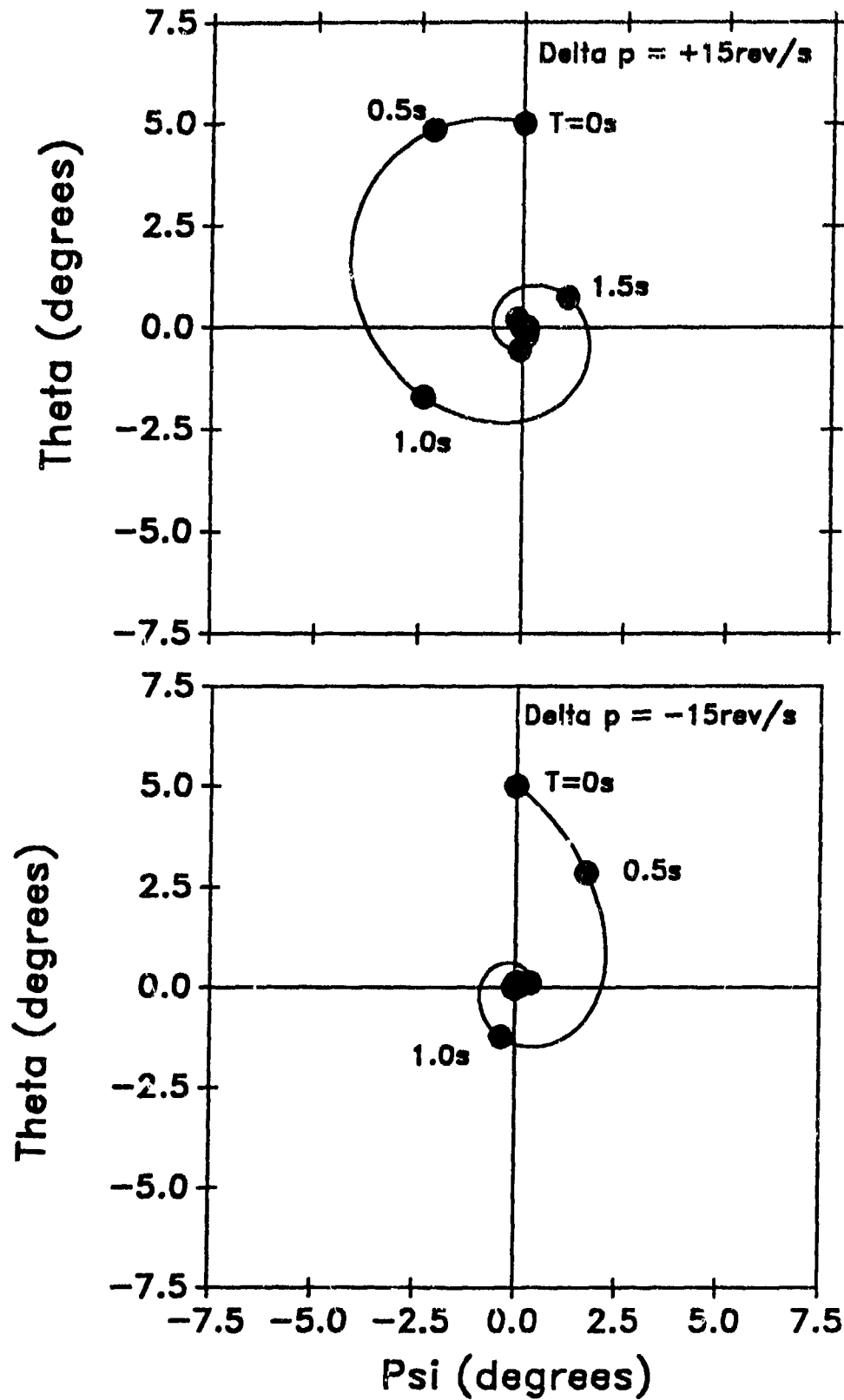


Figure 11: Euler Angle  $\theta$  vs Euler Angle  $\psi$  for Positive and Negative Forward Section Rotation

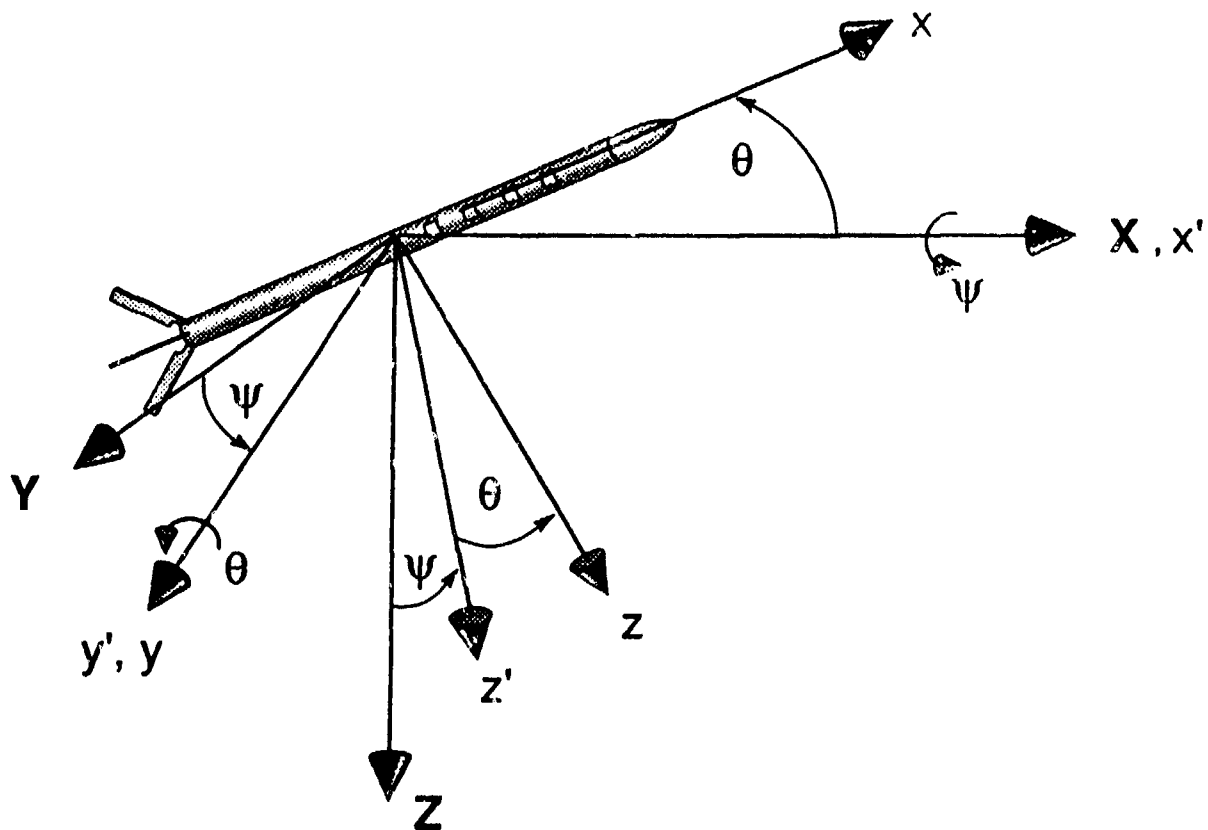


Figure 12: The Bank-Pitch Euler Angle Coordinate System

The advantage of this system is that the angle  $\theta$  is the total angle of attack referred to as  $\Theta$  above. In addition, there is no sideslip angle. This is a convenient system for analysis if the motion is similar to a well behaved top, where the nutation angle stays greater than zero and does not change rapidly. In the Bank - Pitch system, the coordinate  $x$  always points to the nose, the coordinate  $y$  is always normal to the angle of pitch and points to the right when viewed from the back of the missile; the coordinate  $z$  is always in the pitch plane and started out pointing downward before any rolling takes place. This system lends itself the simplest visualization of the aerodynamic forces and moments, and, since the entire cross wind component is contained in the angle  $\theta$ , it is a good system to use for stability analysis.

When the equations of rotation are solved for the highest derivatives, the following equations result:

$$\begin{aligned}\ddot{\phi} &= (\sum T_x - I\ddot{\psi} \cos \theta + I\dot{\psi}\dot{\theta} \sin \theta)/I \\ \ddot{\theta} &= (\sum T_y + (I' - I)\dot{\psi}^2 \sin \theta \cos \theta - I\dot{\psi}\dot{\phi} \sin \theta)/I' \\ \ddot{\psi} &= (\sum T_z + (2I' - I)\dot{\psi}\dot{\theta} \cos \theta - I\dot{\theta}\dot{\phi})/I' \sin \theta\end{aligned}\quad (39)$$

The first equation is for the spin of the missile. The right side of the third equation can be substituted for the  $\ddot{\psi}$  term, which reduces the equation to a single second order derivative. The second equation contains the moments for the pitch plane and determines the total angle of attack, or "nutation" angle. The third equation, for bank, or "precession" angle, is undefined for a total angle of attack,  $\theta$ , equal to zero. This is similar to the gimbal lock problem of a real gyroscope. The disadvantage of this system for long term prediction of rotational motion of a missile is that the nutation angle (pitch) of a missile does change rapidly and sometimes gets very close to zero, or even goes through zero. The former causes very high rates of angular accelerations of the angle  $\psi$ , which slows down the computation; the latter causes the solution to have a divide by zero error. Consequently, the set is useful for the initial portion of the simulation, but cannot be used as  $\theta$  goes to zero.

The typical static stability analysis involves setting all angular rates to zero (except for spin), setting the angle of attack ( $\theta$ ) equal to some small angle, and determining if the angular acceleration in pitch ( $\ddot{\theta}$ ) is positive (unstable), negative (stable), or zero (neutrally stable). With all angular rates equal to zero, the pitch angular acceleration equation reduces to:

$$\ddot{\theta} = \sum T_y/I' \quad (40)$$

The moments in pitch are the following: aero restoring, aero damping, jet damping, and Magnus drag. Magnus lift does not affect the static stability. With zero angular rates, the two damping terms are zero and equation becomes:

$$\ddot{\theta} = (C_{m\alpha}QS\lambda\alpha + \frac{1}{2}\rho Va^2b^2(\Delta p)\sin\alpha)/I' \quad (41)$$

With small angles, the sine of the angle approaches the value of the angle in radians. Since  $a$  is the radius, it is one half the reference length  $\lambda$ , and  $Q$  is  $\rho V^2/2$ . With these substitutions, the equation becomes:

$$\ddot{\theta} = (C_{m\alpha} Q S \lambda \alpha + Q \frac{\lambda^2}{4V} b^2 (\Delta p) \alpha) / I' \quad (42)$$

For a rocket such as REFS, with fins in the rear,  $C_{m\alpha}$  is negative, and, with a positive  $\alpha$ , the contribution of the term is negative. If the forward spin is negative, then the Magnus drag provides another negative term that works with the aero restoring moment to provide additional static stability. If the forward spin is positive, the Magnus drag works against the restoring force and could be destabilizing. This is in agreement with the simulations. Observe the more rapid decrease in angle of attack in Figure 11 when the  $\Delta P$  is negative.

The value of  $C_{m\alpha}$  necessary for neutral stability condition is obtained by setting  $\ddot{\theta}$  to zero:

$$C_{m\alpha} = -\frac{b^2 \lambda (\Delta p)}{S 4V} \quad (43)$$

Note that  $C_{m\alpha}$  is dimensionless except that it is per radian. So long as  $C_{m\alpha}$  is more negative than the expression on the right, the missile is statically stable. Remember that the Magnus drag moment was based on the worst slope of the drag curve, so the analysis is conservative and overpredicts the destabilizing effects for a good part of the flight regime.

Equation (41) indicates that the critical flight condition occurs at minimum velocity. The typical velocity profile for the REFS mission is for the missile to leave the launch tube at about 100 ft/s and rapidly accelerate to 2400 ft/s at burnout. There is a local minimum at apogee of about 140 ft/s. When this minimum and the missile parameters from Table 1 are substituted into the above equation, the minimum magnitude of the coefficient is about 8.3. Recall that the  $C_{m\alpha}$  can be expressed as the product of  $C_{N\alpha}$  times the static margin. At low speeds, this missile has a  $C_{N\alpha}$  of about 9.3. This indicates that the static margin for neutral stability is about 0.88.

The equation for precession (the  $\dot{\psi}$  equation) reinforces the previous observation that the Magnus lift term controls the direction of precession. For the initial condition when the only angular velocity is the spin and the only angle is a small angle of attack, the equation reduces to:

$$\dot{\psi} = \sum T_z / I' \sin \theta \quad (44)$$

With no  $q$  or  $r$  angular velocity, there is no  $z$  damping, so the only moment is the Magnus lift moment:

$$\dot{\psi} = -\rho V a^2 b^2 (\Delta p) \sin \alpha / I' \sin \theta \quad (45)$$

With this coordinate system, the Magnus Lift moment remains along the  $z$  axis and forces the precession in the direction opposite to the sense of the forward relative rotation rate,  $\Delta p$ . A stable missile will begin to develop a negative  $\dot{\theta}$ , adding a positive kinetic term to the  $\dot{\psi}$  equation. Eventually the precession acceleration is balanced by damping terms.

A final stability question that might be addressed is one usually analyzed for tops and gyroscopes: are there any solutions with constant angle of attack (nutation angle) and constant precession rate. Since the gravitational term for a top is always a pure  $T_y$ , the typical top has only very small  $T_z$  terms which are associated with damping of the usually low precession rates. With no  $\dot{\theta}$  terms, and essentially no moments, then the third equation of rotation shows that there will be no change to the precession rate. Then, assuming that there is little or no change to the spin rate, the second equation provides the precession rate required to cancel out the gravitational moment.

For the REFS missile, the static stability is so high that the missile never stays at an appreciable angle of attack for very long. If the static margin were reduced to near neutral magnitudes, then the Magnus lift moment provides a moment in the  $z$  direction, which is not present in top motion. The Magnus lift moment accelerates the precession until balanced by kinetic and damping terms at an equilibrium precession rate. This rate would probably not be the correct precession rate to balance any aerodynamic moments in the nutation equation. Even a top does not automatically find the correct precession rate to eliminate nutation, but must be coaxed into it, which takes a little practice. To find a constant nutation angle solution for missile flight with Magnus lift moments would demand a very contrived set of conditions.

## 4 CONCLUSIONS

The REFS missile will not suffer any problems from Magnus moments. The missile is more aerodynamically stable than typical missiles. If the static margin were reduced to typical levels of 1 to 2, the missile should show no ill effects. The static stability analysis indicated that if the static margin were below 1, some problems could develop at apogee if the  $\Delta P$  is positive. If direction of rotation of the front section relative to the rear is an open choice,  $\Delta P$  should be in the negative sense (counterclockwise looking from the rear). This will provide additional aerodynamic stability.

## References

- [1] Sturek, W.B., Dwyer, H.A., Kayser, L.D., Nietubicz, Reklis, R.P., and Opalka, K.O., (1978) "Computations of Magnus Effects for a Yawed, Spinning Body of Revolution", *AIAA Journal*, Vol. 16, No. 7, p. 687.
- [2] AVCO Systems Division (1974) *MASS Program User's Manual*, AVCO Systems Division, Maryland Operations, Seabrook, Maryland, prepared for NASA Goddard Space Flight Center, Greenbelt Maryland, Contract NAS5-23231
- [3] Shames, I.H., (1980) *Engineering Mechanics, Statics and Dynamics*, 3 ed., Prentice-Hall, Inc., Englewood Cliffs, NJ
- [4] Nelson, R. C., (1989) *Flight Stability and Automatic Control*, McGraw-Hill Book Company, Inc., New York
- [5] Winn, W.P. (1969) National Center for Atmospheric Research, Boulder, Colorado, personal communication.
- [6] Vukelich, S.R., Stoy, S.L., Burns, K.A., Castillo, J.A., and Moore, M.E. (1986) *Missile DATCOM, Volume I - Final Report*, AFWAL-TR-86-3091, Flight Dynamics Laboratory, Air Force Wright Aeronautical Laboratories, Air Force Systems Command, Wright-Patterson Air Force Base, Ohio 45433-6553.
- [7] Hoak, D.E., and Finck, R.D., (1978) *USAF Stability and Control Datcom*, AFWAL TR-83-3048, October 1960, Revised 1978.
- [8] Nielsen, J.N., (1960) *Missile Aerodynamics*, McGraw-Hill Book Company, Inc., New York
- [9] White, F.M., (1979) *Fluid Mechanics*, McGraw-Hill Book Company, NY, p. 476ff.
- [10] Rouse, H. (1946) *Elementary Mechanics of Fluids*, Wiley, NY